Electronic Supplementary Material (ESI) for Molecular Systems Design & Engineering.

Supporting Information

Rheological and Structural Properties of Associated Polymer Networks Studied via Nonequilibrium Molecular Dynamics Simulation

Yuankun Peng[1], Tongkui Yue[2], Sai Li[2], Ke Gao[2], Yachen Wang[2], Ziwei Li[4]*, Xin Ye[1,2,3], Liqun Zhang[1,2,3] and Jun Liu[1,2,3]*

[1]Key Laboratory of Beijing City on Preparation and Processing of Novel Polymer Materials, Beijing University of Chemical Technology, People's Republic of China

[2]Beijing Engineering Research Center of Advanced Elastomers, Beijing University of Chemical Technology, People's Republic of China

[3]State Key Laboratory of Organic-Inorganic Composites, Beijing University of Chemical Technology, 100029 Beijing, People's Republic of China

[4]School of Material Science and Engineering, Guilin University of Technology, Guilin 541004, People's Republic of China

1. Setting of parameters of force-fields and equilibrium conditions

1.1 The non-bonded energy and bonded energy

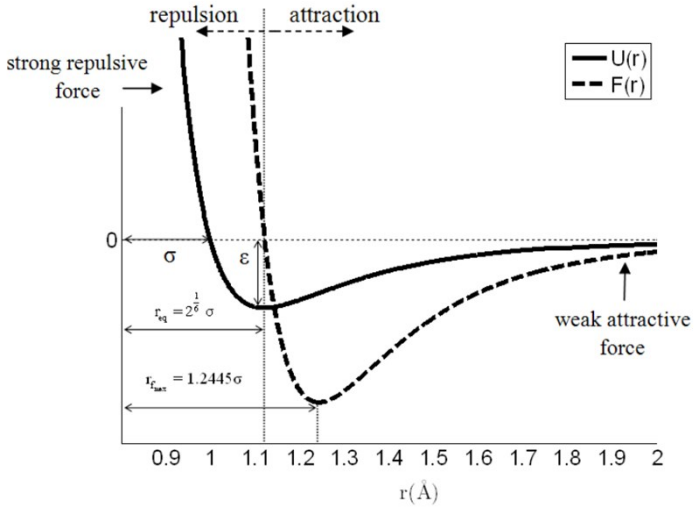

Figure S1. Lennard-Jones potential U(r), and internal force F(r).

The potential energy function describing the interaction between atoms is called the force-fields, including non-bonded interaction (LJ potential) and bonded interaction (FENE potential).

For the non-bonded energy, the most common expressionof the LJ potential is:

$$U_{LJ} = 4\varepsilon\left[(\frac{\sigma}{r})^{12} - (\frac{\sigma}{r})^{6}\right] = \varepsilon\left[(\frac{r_m}{r})^{12} - 2(\frac{r_m}{r})^{6}\right]$$

where ε is the depth of the potential well, σ is the finite distance at which the inter-particle potential is zero, r is the distance between the particles, and the potential function has the lowest value -ε, corresponding to the distance equal to $r_m = 2^{1/6}\sigma \approx 1.12\sigma$. When the distance is less than 1.12σ, the interaction force is positive, and the system beads are in a state of repulsion.

It can be easily verified $U_{LJ}(r_c) = 0$, thus eliminating the jump discontinuity at $r = r_c$. At r = 2.5σ, the Lennard-Jones potential is about 1/60σth of its minimum, ε (the depth of the potential well). Although the value of the (unshifted) Lennard Jones potential at $r = r_c = 2.5\sigma$ is rather small, the effect of the truncation can be significant.

So that the LJ potential is cut off at different distances to model the attractive or repulsive interactions in our simulation. The repulsive interactions are simulated by setting $r = r_c = 2.5\sigma$, whereas $r_{cutoff} = 2 \times 2^{1/6}\sigma = 2.24\sigma$ and $r_{cutoff} = 2.5\sigma$ represent a simulated short-ranged attraction and a long-ranged attraction, respectively. Since each bead describes 3-6 monomers in the molecule dynamics simulation, r_{cutoff} is in the nanometer range.

The cutoff distance between the main chain beads, and between the main chain beads and the ending beads is set to 1.12σ, which makes them repulsive. In the molecular dynamics simulation of polymer fluids, researchers almost set it like this, including Professor Kroger.[1-6]

On the other hand, originally, it is difficult to achieve equilibrium to calculate the viscosity, especially at a small shear rate. Setting the repulsion will greatly save the calculation time, and regardless of the repulsion or attraction interaction, the qualitative results of the systems will not be influenced. It will only affect the corresponding viscosity value, which happens to be not what we are concerned about. The interaction strength between the main chain beads, and between the main chain beads and the ending beads is set to 1.0ε, which is more similar to a standard parameter, and a lot of research works are based on this.[7, 8]

The cutoff distance between ending beads is set to 2.5σ, it can ensure that there is a long-range attraction between them, which is consistent with the real system, as well as allows ending beads to attract each other through the hydrogen bond, coordination, dipole and other non-covalent bonds interaction. Thus, the ending beads are associated to form a physical polymer network, and different terminal interaction strengths are used to simulate different kinds of non-covalent bonds or functional groups with different magnitude of interaction such as hydroxyl, carboxyl, amino and epoxy groups. For the single chain length systems, we observe that only when the terminal interaction strength exceeds 4.0ε, can the system form a relatively complete physical network. Therefore, for the bimodal molecular weight distribution system, we choose the terminal interaction strength to be 8.0ε to ensure the integrity of the network, which is

beneficial to the following research. At the same time, it should be noted that we do not consider whether they are between the same chain lengths for all the above statements, that is to say, even if the cutoff distance between polymer ending beads with different chain lengths is 2.5σ, the other parameters are the same.

For the bonded interaction (FENE potential), because the polymer bead is a rigid sphere with diameter of 1σ, the nearest distance between the mass centers of the two beads is 1σ, so we set the maximum bond length R_0 to 1.5σ, which ensures that it greater than 1σ, and set the spring constant K to $30\varepsilon/\sigma^2$. For this choice of parameters, the maximal extent of bonds is short enough to prevent crossing of chains, whereas the magnitude of the bonding force is small enough to enable simulations with relatively large time steps.

1.2 The setting of equilibrium conditions

For the setting of equilibrium conditions, we set the temperature to 1.0, because we follow the work of Kremer and Grest who studied polymeric systems,[9] and a lot of research works are based on this.[5, 8]

We set the pressure at about 4.5 to ensure that the number density of the system is 0.84, which is an appropriate density to correspond to the density of polymer melt.[10]

The time step is set to 0.001τ, because too large time step will make the simulation results inaccurate and cause atoms to overlap with errors. Too small time step will make the running time longer, so we need to choose an appropriate time step. These parameter settings can be found in the previous work of our group or other groups.[6, 8, 11, 12]

2. The verification of simulated results using experimental data

We first studied the effect of the chain length on the rheological properties, and the results showed that the large chain length system possesses the greater zero-shear viscosity and the stronger shear thinning behavior. The chain length corresponds to the molecular weight of the real polymer. In the experiment, the influence of molecular weight on shear thinning is also very simple. The researchers have done a lot of thorough research on it, so we will not repeat it too much. For example, Hadjistamov et al.[13] studied the viscosity curves of silicone oil with molecular weights of 20000,

50000, 80000, 100000 and 500000, and obtained the same qualitative results as our simulations. In addition, the power law exponent we calculated is in the range of 0.35-0.85, which is actually very approaching to the experimental value of linear polyethylene melt ($0.4<n<0.9$).[14]

For changing the interaction strength between the terminal functional groups $\varepsilon_{end\text{-}end}$, when $\varepsilon_{end\text{-}end}$ is large enough, the physical network structure can be formed by the attraction interaction between the ending beads. Different $\varepsilon_{end\text{-}end}$ can correspond to the different non-bonded interactions such as Van der Waals force, dipole, hydrogen bond and coordination in the experiment or different functional groups such as hydroxyl, carboxyl, amino, epoxy groups, etc., so it can provide reference for the experimental study of the influence of different kinds of interactions on the rheological properties of the systems. For example, Peng et al.[15] studied the rheological behavior of novel dendron hydrophobically modified ethoxylated urethanes with almost the same molecular weights, molecular weight distributions and identical hydrophilic portion but different terminal hydrophobic group numbers. The results show that the system with more terminal hydrophobic groups forms a more complete physical network, exhibits a relatively higher solution viscosity, and exhibits more pronounced shear thinning behavior.

As for the bimodal molecular weight distribution (MWD) systems, we used a novel method to design the equivalent average molecular weight of the two peaks in the actual system with two chain lengths. As mentioned in the introduction of our paper, many researchers have studied commercial bimodal polyethylene by experiments, but no one has explored the end-functionalized bimodal MWD system. For example, Wu, Liu, Shen, etc.[16, 17] have all studied the rheological behavior of bimodal MWD Polyethylene (PE). Shen et al.[18] obtained bimodal MWD polymer by blending low-molecular-weight PE and high-molecular-weight PE in different proportions in xylene solution, and oscillating shear experiments show that the zero-shear viscosity increases as the proportion of high molecular weight increases. Wu et al[19] obtain similar results that low molecular weight components can reduce the melt viscosity. However, our

simulated results are contrary to their work, but this is not a contradiction, because the physical network is formed in our system due to the interaction of the end functional groups, and the effect of end functional groups on the physical properties has also been studied in other literatures. For example, Krakovsky et al.[20] studied dihydroxy terminated polybutadienes of different molecular weights, and DSC results show that the polybutadiene with larger molecular weight has a lower glass transition temperature, which is also the result of the inversion caused by the physical network formed in the system, it indirectly proves the accuracy of our results.

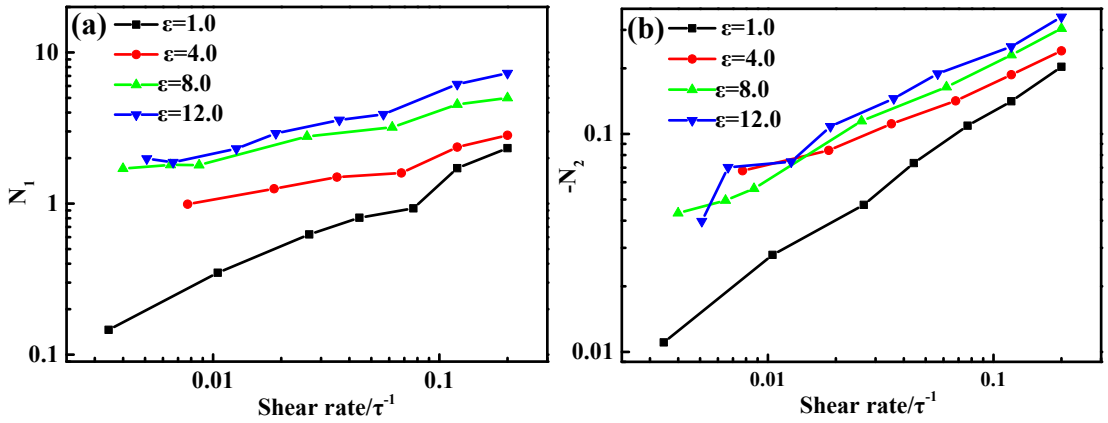

Figure S2. (a) The first normal stress difference N_1 (b) negative second normal stress difference $-N_2$ as a function of shear rate for different terminal interaction strengths.

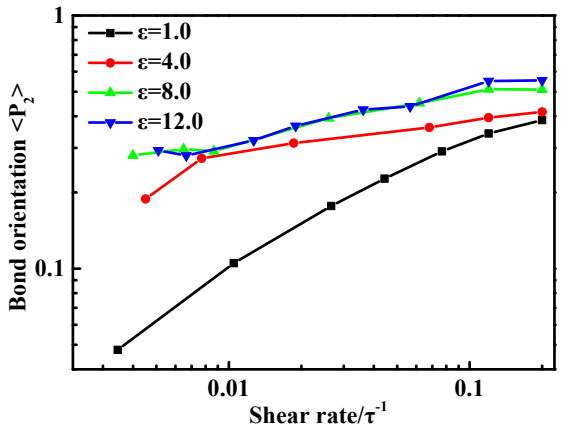

Figure S3. The bond orientation $<P_2>$ for different $\varepsilon_{end\text{-}end}$ as a function of shear rate.

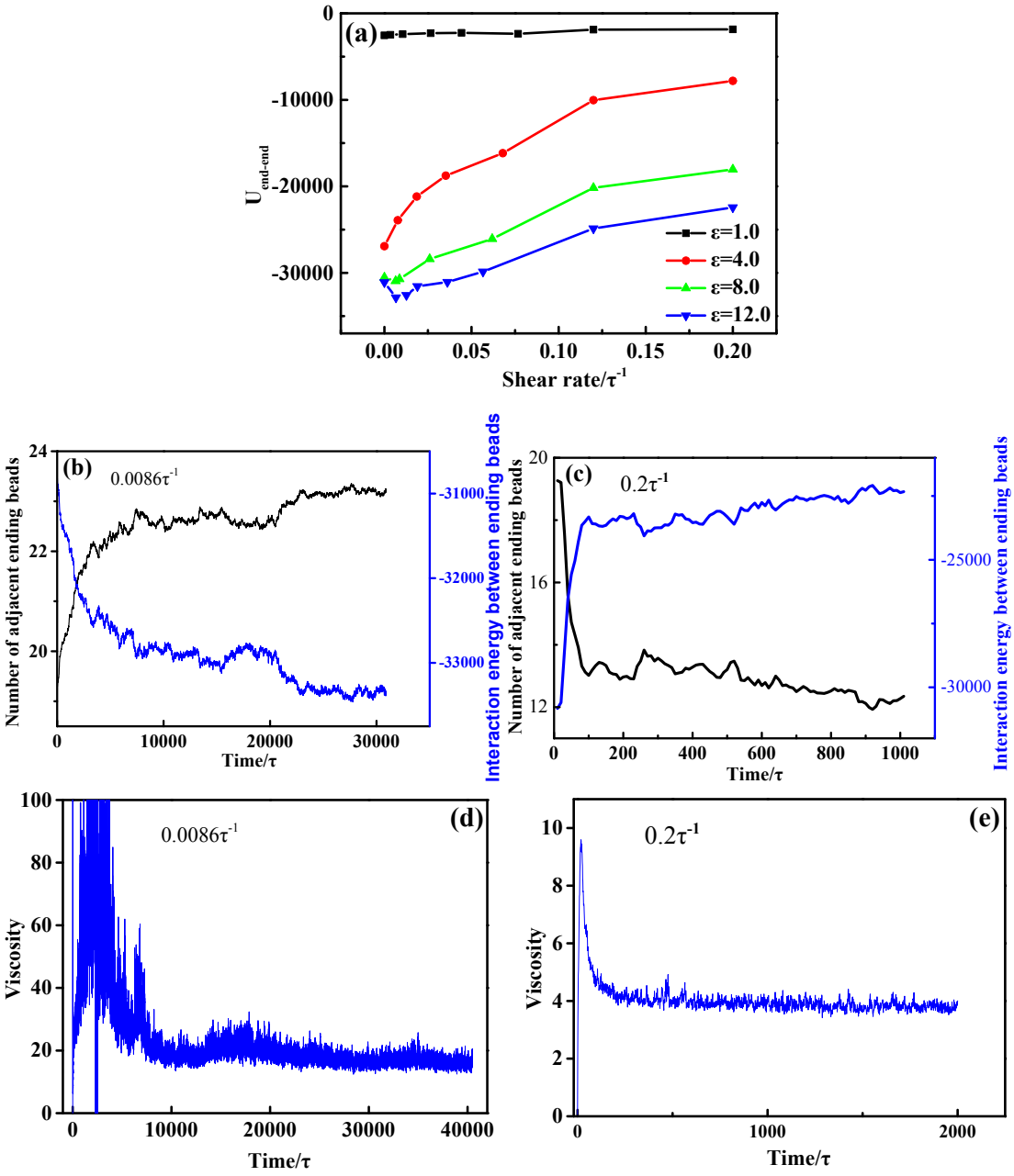

Figure S4. (a) The non-bonded interaction between ending beads $U_{end-end}$ during shear for different terminal interaction strengths systems. The number of adjacent ending beads and interaction energy between ending beads as a function of time for ε=12.0 system at (b) shear rate 0.0086τ^{-1} and (c) 0.2τ^{-1}. The viscosity as a function of time for ε=12.0 system at (d) shear rate 0.0086τ^{-1} and (e) 0.2τ^{-1}.

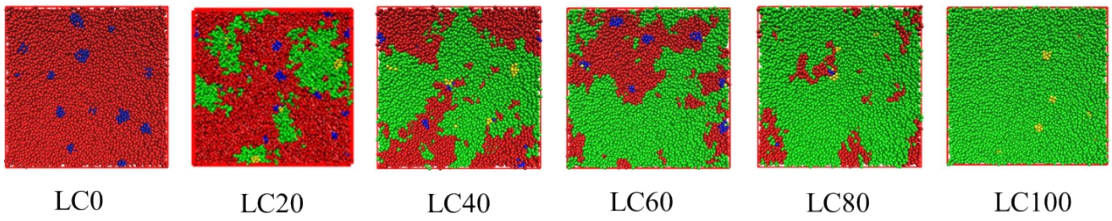

Figure S5. The snapshots of equilibrium systems for different proportion of long chain.

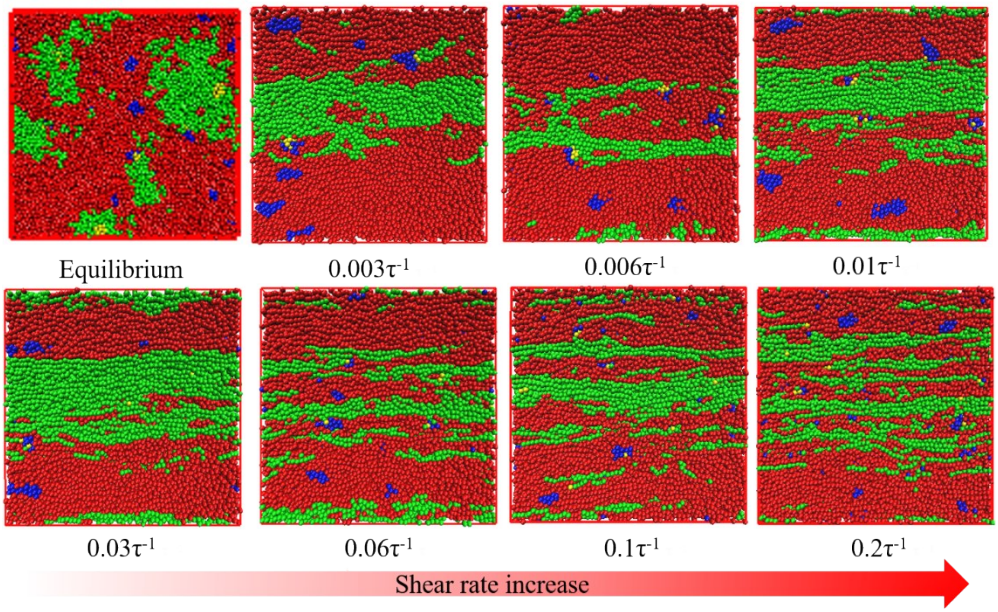

Figure S6. The snapshots of LC20 system at equilibrium and different shear rates.

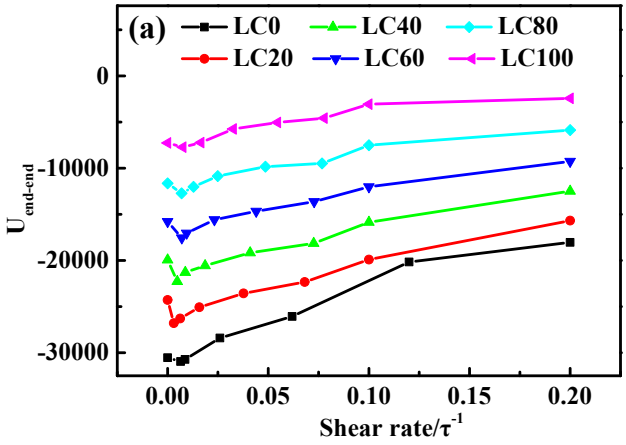

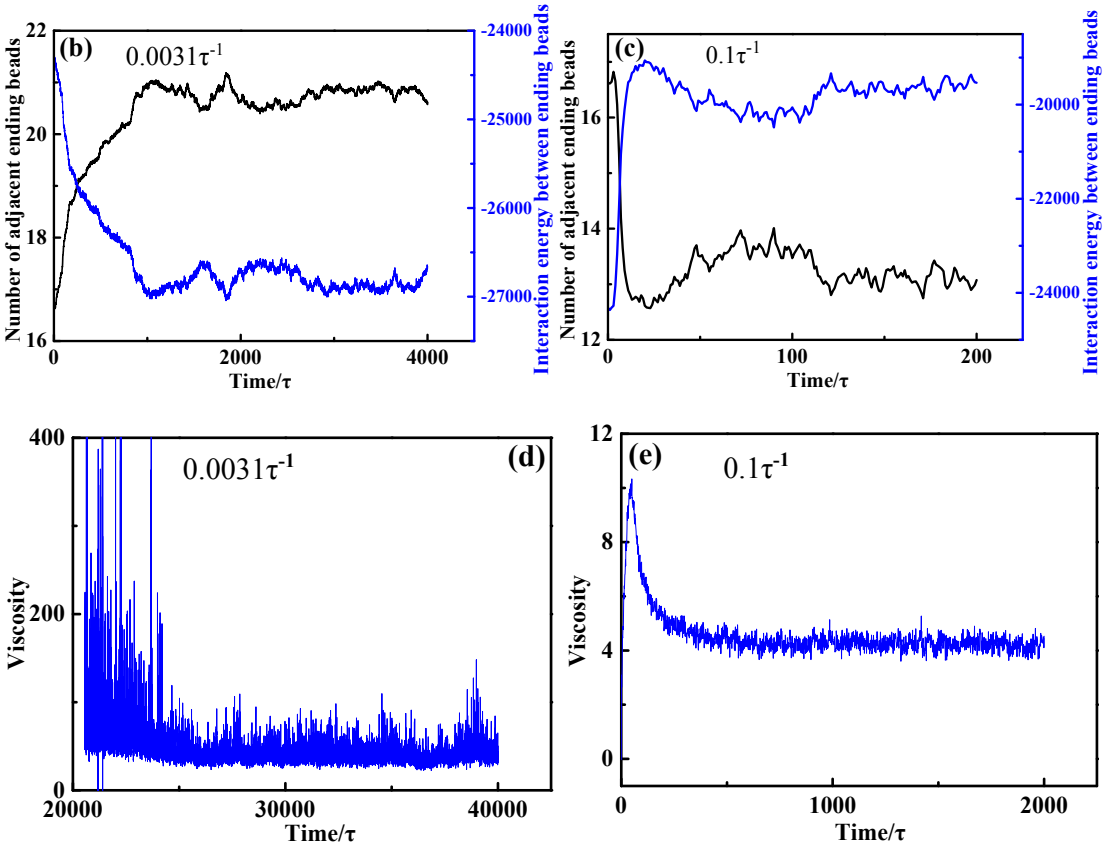

Figure S7. (a) The non-bonded interaction between ending beads $U_{end\text{-}end}$ during shear for different φ systems. The number of adjacent ending beads and interaction energy between ending beads for LC20 system at shear rate (b) $0.0031\tau^{-1}$ and (c) $0.1\tau^{-1}$. The viscosity as a function of time for LC20 system at shear rate (d) $0.0031\tau^{-1}$ and (e) $0.1\tau^{-1}$.

References

1. H. Guo and K. Kremer, *Journal of Chemical Physics*, 2007, **127**, 1856.
2. K. Hagita, T. Murashima, H. Takano and T. Kawakatsu, *Journal of the Physical Society of Japan*, 2017, **86**, 124803.
3. E. Hajizadeh, B. D. Todd and P. J. Daivis, *Journal of Rheology*, 2014, **58**, 281-305.
4. M. Kröger and S. Hess, *Physical Review Letters*, 2000, **85**, 1128-1131.
5. Kröger and Martin, *Journal of Rheology*, 1993, **37**, 1057-1079.
6. X. Xu, J. Chen and L. An, *The Journal of Chemical Physics*, 2014, **140**, 174902.
7. J. S. S. A, D. B. A and G. D. S. A. B, *Composites Science and Technology*, 2003, **63**, 1599-1605.
8. S. Li, Z. Zhang, G. Hou, J. Liu, Y. Gao, P. Coates and L. Zhang, *Physical Chemistry Chemical Physics*, 2019, **21**, 11785-11796.
9. K. Kremer, G. S. Grest and I. Carmesin, *Physical Review Letters*, 1988, **61**, 566-569.

10. K. Kremer and G. S. Grest, *Journal of Chemical Physics*, 1990, **92**, 5057-5086.
11. H. Wan, K. Gao, S. Li, L. Zhang, X. Wu, X. Wang and J. Liu, *Macromolecules*, 2019, **52**, 4209-4221.
12. Z. Zhang, J. Liu, S. Li, K. Gao, V. Ganesan and L. Zhang, *Macromolecules*, 2019, **52**, 4154-4168.
13. D. Hadjistamov, *Journal of Applied Polymer Science*, 2008, **108**, 2356-2364.
14. Hassager, *Dynamics of polymeric liquids*, Dynamics of polymeric liquids, 1987.
15. J. Peng, R. Dong, B. Ren, X. Chang and Z. Tong, *Macromolecules*, 2014, **47**, 5971-5981.
16. H. Liu, E. M. Troisi, J. Goossens, J. R. Severn and C. Bastiaansen, *Journal of Applied Polymer Science*, 2019, 136, 74577.
17. H. W. Shen, B. H. Xie, W. Yang and M. B. Yang, *Journal of Applied Polymer Science*, 2013, **129**, 2145-2151.
18. H. W. Shen, L. Tao, B. H. Xie, Y. Wei and M. B. Yang, *Journal of Applied Polymer Science*, 2011, **121**, 1543-1549.
19. T. Wu, L. Yu, Y. Cao, F. Yang and M. Xiang, *Journal of Polymer Research*, 2013, **20**, 1-10
20. Krakovsky, I., Hanykova, L., Trchova, M., Baldrian, J. and Wubbenhorst, *Polymer London*, 2007, 48, 2079-2086.